International Conference on
Environmentally Sound Water Resources Utilization
Bangkok, Thailand, 8-11 November 1993

A STUDY OF RUN-OFF MODELS CONSIDERING GROUND WATER FLOWS

Yoshiteru ICHIKAWA
Yasuyuki SHIMIZU
Tosihito TOYABE

Civil Engineering Research Institute, 062 Hiragishi 1-3
Toyohiraraku Sapporo, Japan

ABSTRACT

Establishing the physical mechanism of rainfall and runoff in catchment areas is important for the maintenance of catchment areas and rivers. Presently, the concentration-type models generally used in river planning (such as the hydrograph analysis by storage functions) represent these phenomena with adjustable parameters, but do not evaluate their physical significance. A distribution-type runoff model which represents the physical mechanisms is needed to incorporate the varying conditions of catchment areas. Such a model is presented in this study with a model of saturated and unsaturated percoration flows using the Richards' Equation to represent the rainfall and runoff mechanism on slopes. This model is verified by comparing it with the rainfall percolation runoff experiments on two-dimensional slopes.

INTRODUCTION

This study aims to establish runoff characteristics by measuring pore water pressures and runoff discharges in soil layers. It also develops a model of saturated and unsaturated seepage flows using the Richards' Equation to represent the rainfall and runoff mechanism on slopes, and investigates characteristics of the model by comparing rainfall·seepage·runoff experiments on two-dimensional slopes.

EXPERRIMENTAL INSTRUMENTATION

The experimental instruments consist of a soil layer, a rainfall generation facility, and a runoff as shown in Figure-1, as well as a data display and storage facility. The functions, sizes, and characteristics are as follows: The soil layer uses a tilting flume, 30cm wide, 500cm long, and 40cm deep, filled with quartz sand (particle size ϕ=0.2mm) in the 480cm-long slope and gravel in the 20cm-long downstream end to prevent quartz sand from being washed out. Tensiometers are installed at 21 points in the sidewall for pressure measurements. For the rainfall generation, three vinyl chloride pipes are placed in the direction of the slope, with 0.4mm holes at 5cm intervals and hanging cotton threads are used to form raindrops to simulate rainfall. A net to break the fall of the drops is set slightly above the soil layer to prevent the development of cavities

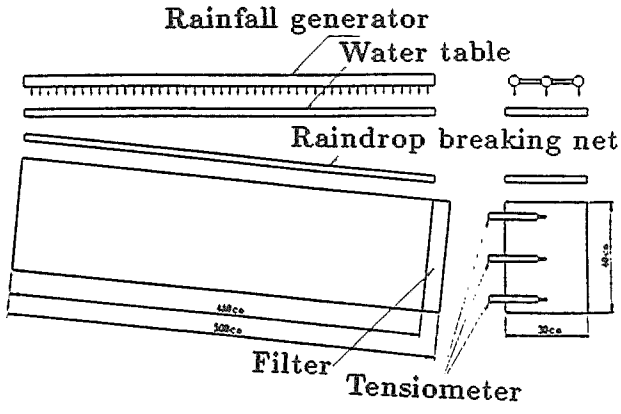

Figure-1 Experimental Installation

on the soil layer and to distribute the water widely. To supply a set rainfall volume, tap water is stored in a water tank, and supplied while maintaining a stable water level in the tank. The rainfall intensity is controlled by a valve attached to each vinyl chloride pipe. A runoff counter is set at the runoff, and measures runoff per unit time, which is then accumulated. To determine the accuracy of the runoff counter, a tipping-bucket rain gauge is also placed to measure the runoff discharge. The data display and storage reads data from the tensiometers and the runoff counter at set time intervals for predetermined periods, displays it on a personal computer, and stores it on a hard disc.

OUTLINE OF EXPERIMENTS

The experiment was conducted for four conditions with rainfall intensities of 10mm/hr and 30mm/hr on 1/5 and 1/10 slopes. Immediately before the start of the experiment, the data display and storage was reset. The rainfall intensity was controlled in each experiment, and determined by averaging three measurements. Data was read at one-minute intervals, and the completion time was based on experiments conducted the previous year. The data obtained from the experiment is comprised ofthe negative soil pressure (suction ψ) at 21 measuring points (arrangement shown in Figure-2) and the accumulated runoff. The values were stored on a hard disc, and displayed on a monitor as a volt-time graph. The water was stopped depending on the progress of the experiment, after the runoff had reached a steady state.

In some cases, there was surface runoff, and this was measured per minute with a measuring cup. After the rainfall had been stopped, measurement of the negative pressure and runoff discharge continued for a set time. Before the start of experiments, the soil was drained to a uniform initial condition.

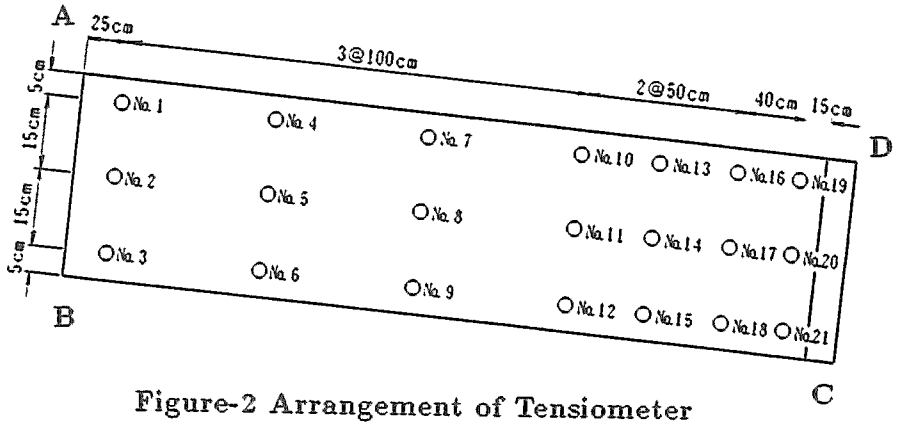

Figure-2 Arrangement of Tensiometer

Table-1 Experimental Conditions

case-no.	Gradient	Rainfall time (hr)	Rainfall intensity (mm/hr)	
			Start	Stop
1	1/5	6.0	10.72	10.44
2	1/10	8.0	10.90	10.26
3	1/5	4.5	30.85	29.63
4	1/10	3.0	32.05	30.46

EXPERIMENTAL RESULTS AND DISCUSSION

Figure-3 to -10 show hydrographs of runoff discharges and changes in suction with time. Figures-3, -5, -7, and -9 represent the infiltraiton discharge [q_1 (mm/hr)], the surface discharge [q_2 (mm/hr)],

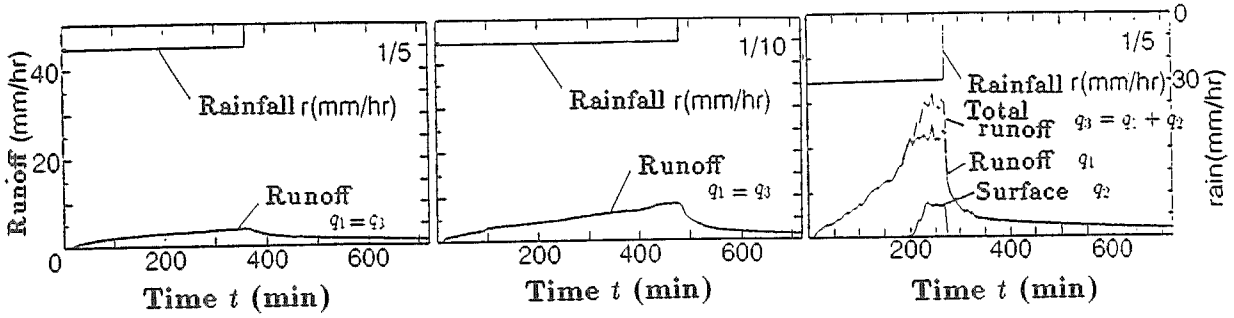

Figure-3 Changes in Rainfall Intensity r and Runoff (Case 1)

Figure-5 Changes in Rainfall Intensity r and Runoff (Case 2)

Figure-7 Changes in Rainfall Intensity r and Runoff (Case 3)

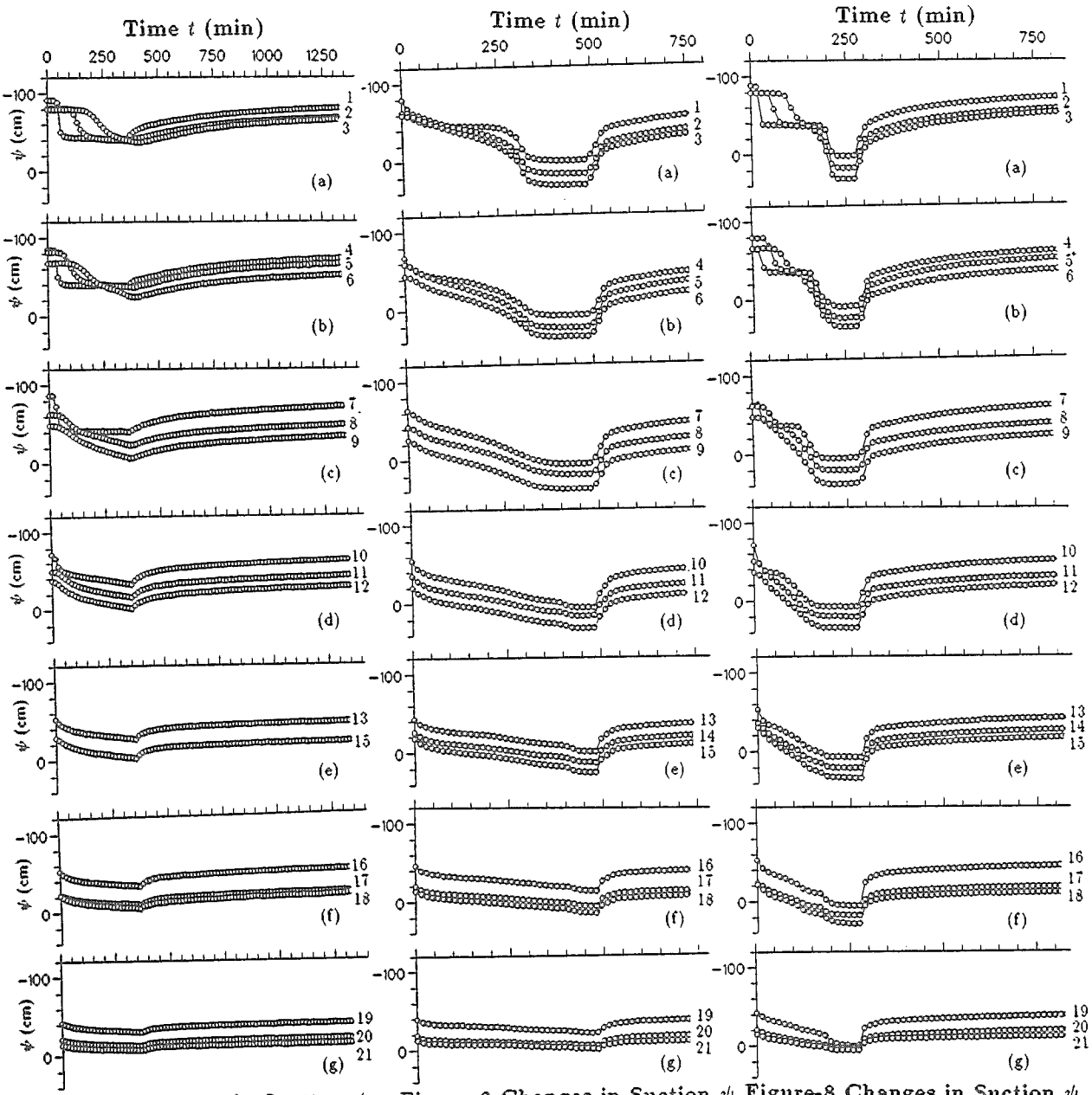

Figure-4 Changes in Suction ψ (Case 1)

Figure-6 Changes in Suction ψ (Case 2)

Figure-8 Changes in Suction ψ (Case 3)

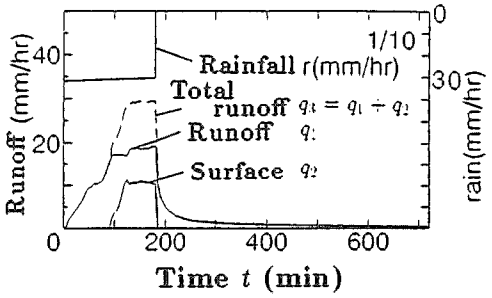

Figure-9 Changes in Rainfall Intensity r and Runoff (Case 4)

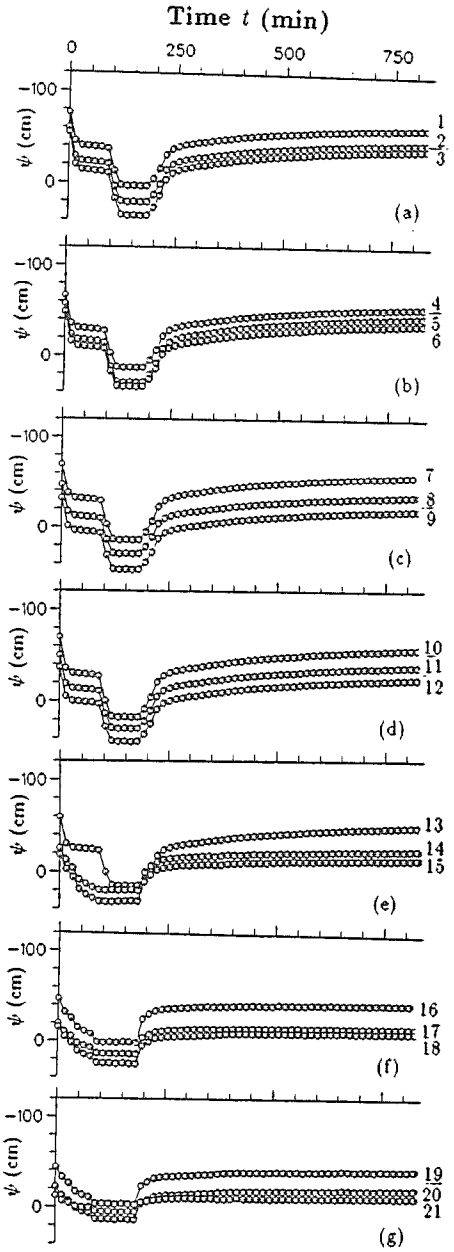

Figure-10 Changes in Suction ψ (Case 4)

and the total discharge [q_3 ($= q_1 + q_2$)]. Numbers at the lines in Figures-4, -6, -8, and -10 refer to the positions of the tensiometers in Figure-2.

All hydrographs show that the runoff occurs after the start of rainfall and continues for a while after rainfall has stopped, and that the runoff discharge decreases rapidly after rainfall has stopped. The time lag of the runoff at the downstream end after discontinuing the rainfall may be caused by water stored before it leaves the soil water as runoff. A rapid decrease in runoff discharge after the stop of rainfall may be caused by the rainfall intensity being inadequate to force out the soil water. The suction pressure falls rapidly to negative values in all cases. It is not likely that the behavior of soil water changes rapidly like this, and this observed change may be due to the differences in the water content and suction pressures in the absorption and drainage processes (a hysteresis phenomenon).

With 30mm/hr rainfall, the runoff increases stepwise till a steady state. The suction also changes stepwise to positive before reaching the steady state. The time for both runoff discharge and suction to change to the steady state are similar. This phenomenon occurs only with rainfall, and may be due to infiltration of rainfall. Pores in the soil fill partly with rain water and may improve the permeability of the soil, and further increase the runoff discharge. An increase in runoff discharge does not cause a sudden change to positive suction, but the suction values show positive changes. This arises due to an increase in discharge from the ground surface drawn by the runoff at the downstream end, as well as an increase in permeability.

With a rainfall intensity of 30mm/hr on both 1/5 and 1/10 slopes, the total runoff discharge is equal to the rainfall intensity, and the soil layer is saturated at the steady state. The time to reach the steady state with the 1/10 slope is shorter than that with the 1/5 slope. This may be due to differences in the initial water content and the gravity drainage which is affected by the difference in slope gradients. The steeper slope has a higher ratio of infiltration runoff. This may be cavsed by the pressure gradient in the infiltration runoff.

SATURATED AND UNSATURATED MODELS OF SEEPAGE FLOWS

The experimental results were simulated by calculations using the saturated and unsaturated infiltration theory of Richards'[1)]

The continuity equation of soil water content is expressed by:

$$\frac{\partial \theta}{\partial t} = -\left(\frac{\partial V_x}{\partial x} + \frac{\partial V_z}{\partial z}\right) \tag{1}$$

here x refers to the slope direction along the ground surface, and z to the downward direction perpendicular to the x axis. V_x and V_z are the x and z components of infiltration flow velocities, θ the water content by volume, and t the time; V_x and V_z are given according to the Darcy's law as:

$$V_x = -K\frac{\partial \phi}{\partial x}, \quad V_z = -K\frac{\partial \phi}{\partial z} \tag{2}$$

here ϕ and K refer to the total head and the hydraulic conductivity. When (2) is substituted into (1), the left side of (1) is expressed by :

$$\frac{\partial \theta}{\partial t} = \frac{\partial \theta}{\partial \psi}\frac{\partial \psi}{\partial t} \tag{3}$$

and when the specific water capacity $C(\psi) = \partial\theta/\partial\psi$ is given, (1) is expressed by:

$$C\frac{\partial \psi}{\partial t} = \frac{\partial}{\partial x}\left(K\frac{\partial \phi}{\partial x}\right) + \frac{\partial}{\partial z}\left(K\frac{\partial \phi}{\partial z}\right) \tag{4}$$

Assuming a slope gradient $=\alpha$, the total head ψ is given by:

$$\phi = \psi - x\sin\alpha - z\cos\alpha \tag{5}$$

When ϕ is converted into ψ, (4) is expressed by:

$$C\frac{\partial \theta}{\partial t} = \frac{\partial}{\partial x}\{K\left(\frac{\partial \psi}{\partial x} - \sin\alpha\right)\} + \frac{\partial}{\partial z}\{K\left(\frac{\partial \psi}{\partial z} - \cos\alpha\right)\} \tag{6}$$

The relations between $\psi \sim \theta(\psi)$ and $\psi \sim K(\psi)$ are expressed by Tani's equation:

$$\theta = (\theta_s - \theta_r)\left(\frac{\psi}{\psi_0} + 1\right)exp\left(-\frac{\psi}{\psi_0}\right) + \theta_r \tag{7-1}$$

$$K = K_s S_e{}^{\beta} \tag{7-2}$$

C in (6) uses the following equation, obtained by partially differentiating (7-1) with respect to ψ:

$$C(\psi) = -(\theta_s - \theta_r)\frac{\psi}{{\psi_0}^2}exp\left(-\frac{\psi}{\psi_0}\right), \quad [\psi = \psi'(\psi' \leq 0), \quad \psi = 0(\psi' > 0)] \tag{8}$$

S_e is the effective degree of saturation, and defined as:

$$S_e = \frac{\theta - \theta_r}{\theta_s - \theta_r} \tag{9}$$

here θ is the saturated water content; θ the water content assuming little movable water; ψ the pressure head to give the maximum specific water capacity C; K the saturated hydraulic conductivity; and β the gradient of unsaturated hydraulic conductivity in the unsaturated domain.

The boundary conditions are expressed with A, B, C, and D in Figure-2. Flows passing through the AB and BC surfaces have zero velocity, through CD there is the free outflow, and through AD it is the condition that rainfall is absorbed, these boundary conditions are given by:

$$V_x = 0 \ \text{(AB)}, \quad V_z = 0 \ \text{(BC)}, \quad \frac{\partial V_x}{\partial x} = 0 \ \text{(CD)}, \quad V_z = r(t)\cos\alpha \ \text{(AD)} \tag{10}$$

where $r(t)$ is the rainfall intensity.

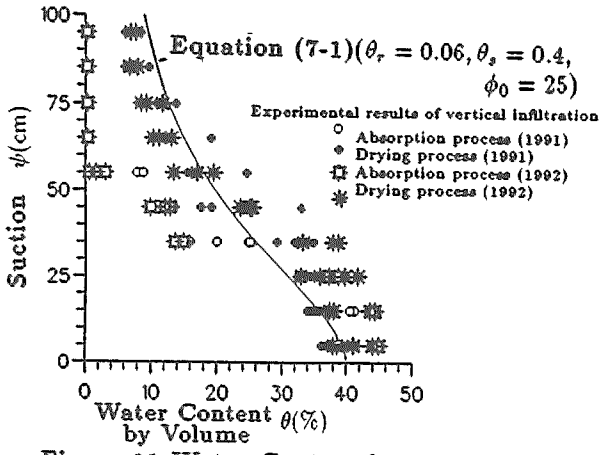

Figure-11 Water Content by Volume θ versus Suction ψ

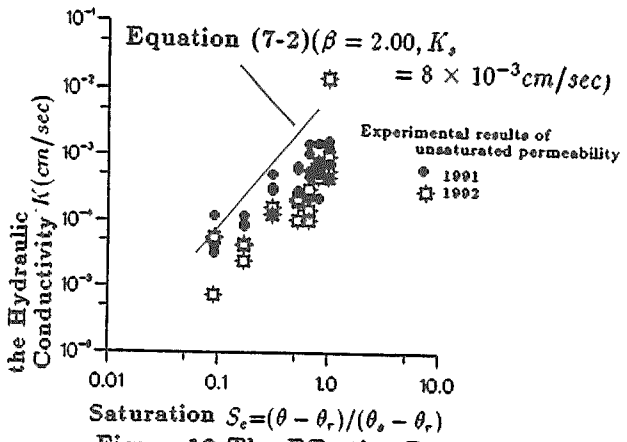

Figure-12 The Effective Degree of Saturation S_e versus the Hydraulic Conductivity K

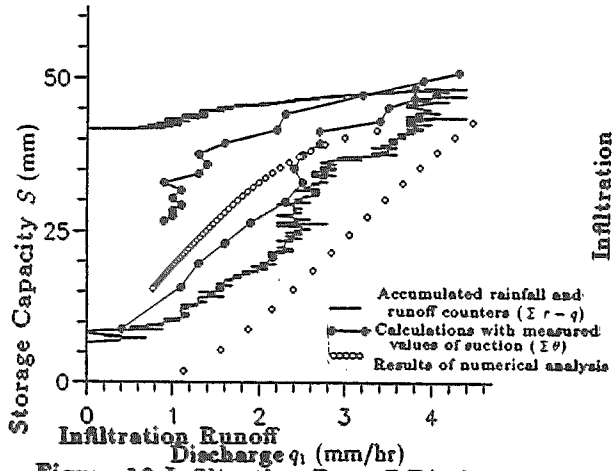

Figure-13 Infiltration Runoff Discharge q_1 versus Storage Capacity S(Case 1)

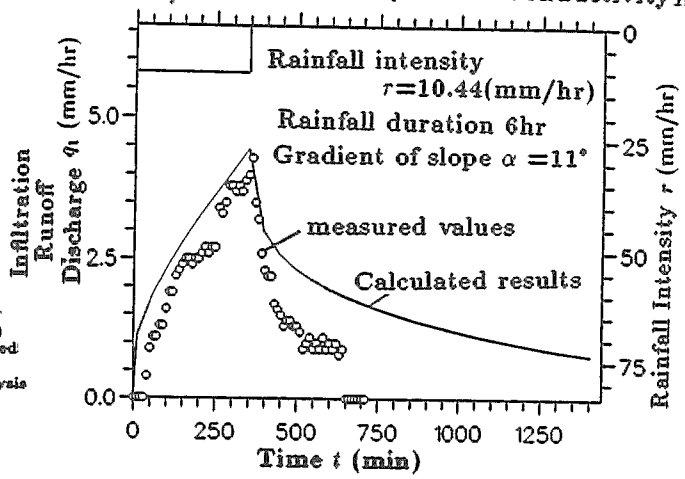

Figure-14 Changes in Rainfall Intensity r and Infiltration Runoff Discharge q_1(Case 1)

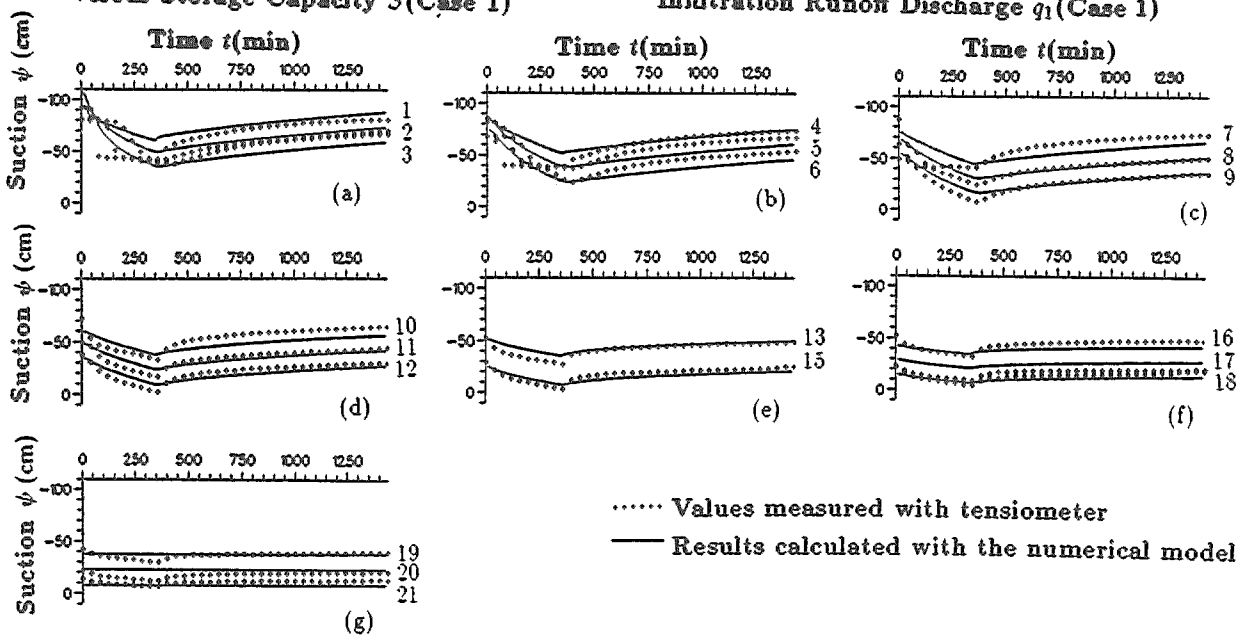

Figure-15 Changes in Suction ψ (Case 1)

DISCUSSION AND COMPARISON OF MEASURED AND MODEL VALUES

Calculated results with the above model under the conditions of case 1 are compared with the experimental results. Calculations of case 1 without surface runoff assumes that all rainfall infiltrates through the ground surface.

To investigate the permeability characteristics of the experimental sand, vertical infiltration and unsaturated permeability tests were conducted. Figure-11 shows the relation between the water content by volume θ obtained with the vertical infiltration test and the suction ψ The preliminary calculations give θ_r =0.06, θ_s =0.40, and θ_0=25cm as parameters in equation (7-1) (shown in Figure-11). The hydraulic conductivity at each suction value is given by the unsaturated permeability test and is converted into the relation between the effective saturation degree, S_e , and the hydraulic conductivity, K, by using the relation between θ and ψ in Figure-11, and the results are shown in Figure-12. The relation between the effective saturation degree, S_e , and the measured hydraulic conductivity, K, in Figure-12 gives β=2.00 and K =8 $\times$ 10^{-3} (cm/sec) as the parameter in (7-2); it is also shown in Figure-12.

A numerical analysis was conducted under the experimental conditions of case 1 using the above parameters. The experimental slope was divided into ten equal parts in the x and z directions, and the differentiation of (6) was made by the Crank Nicolson method.

Figure-13 shows the relation between the infiltration runoff discharge, q_1 , and the storage capacity, S_e. The three kinds of curves in Figure-13 refer to (a) the accumulated differences between the measured rainfall and runoff, (b) the measured suction converted into the water content by volume using eq. (7-1) and integrated, and (c) the calculated values of the numerical model. The lines curve counterclockwise, and the (a) and (b) measurements show that runoff does not occur at the initial stage of rainfall but after the storage capacity has reached some level; (c) the calculations show that both runoff and storage capacity start to increase immediately after rainfall occurs. This result arises because the numerical model uses the boundary condition of free runoff at the downstream end, and even a little storage capacity causes runoff. This shows that the boundary conditions and the equation between θ and ψ may not accurately represent the situation. The general characteristics of the $S\sim q$ curve and the peak discharge and peak storage capacity are well reproduced by the numerical model.

Figure-14 shows measured and experimental results of changes in infiltration runoff discharge. It also represents the characteristics of runoff as in the $S\sim q$ curves. There are large differences between measured and experimental results after the stop of rainfall, possibly due to the equation for θ and ψ in dehydration. It may show the limits of expressing the relation between θ and ψ, which is not originally one-valued, with a one-value function as shown in Figure-11.

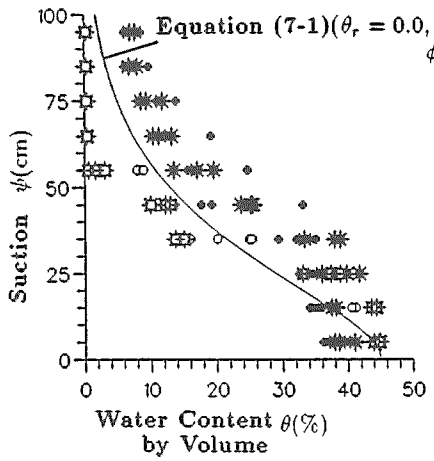

Figure-16 Water Content by Volume θ versus Suction ψ

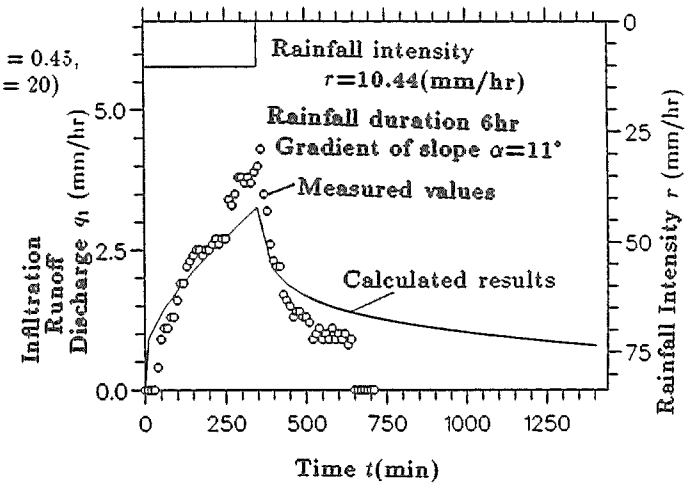

Figure-17 Changes in Rainfall Intensity r and Infiltration Runoff Discharge q_1(Case 1)

Figure-15 compares the calculated and measured results of the changes in suction ψ. Generally, the calculated results agree well with measured values except for differences at the upstream side [(a), (b)]. Figure-13, -14 and, -15 show that the model provides a very accurate calculation of the suction, but a very inaccurate conversion of suction into water content by volume. This may be

because the validity of θ and ψ is not large as mentioned above.

Basically, it is necessary to reformulate the model, integrating the conversion equation and considering the two values in the calculation. To investigate the influence of the differences in the equation between $\theta \sim \psi$on the calculated results, the numerical calculation was also done after changing the equation as shown in Figure-16.

The equation between $\theta \sim \psi$ in Figure-16 attaches more importance to the absorption process than in Figure-11. This leads to the hydrograph of infiltration flows in Figure-17 where the agreement of the calculated results with the measured values in the rising stage (the absorption process) is improved. Compared with Figure-14, however, the agreement with the peak runoff discharge becomes poorer. Calculated results of suction in Figure-16 are equally as good as those in Figure-15. The relation between $\theta \sim \psi$ is important in improving the accuracy of the calculated runoff discharge.

SUMMARY

This study investigated the characteristics of runoff in relation to the gradient of slope and rainfall intensity by performing rainfall and infiltration experiments on a two-dimensional slope. The experiments verified the general characteristics of runoff for rainfall and gradient of slope, and also showed noteworthy phenomena: when surface runoff occurs due to heavy rainfall, the runoff discharge and suction changes stepwise; the runoff discharge on the steeper slope increased at a lower rate than on the gentler slope, but it was larger at the peak runoff discharge (steady-state).

Next, by comparing results of calculations, it was verified that the experimental results of suction in the soil could be satisfactorily reproduced, and that calculated results of infiltration runoff discharge depended largely on the relation between $\theta \sim \psi$. It is appearently necessary to integrate the relation between$\theta \sim \psi$ considering both absorption and drying in the model. Further investigation is required however to determine the spatial and temporal transition from the absorption to drying processes.

The numerical model was applied only to the case without surface flow. Further investigation is necessary to determine the boundary conditions on the ground surface with surface flows.

REFERENCE

1) Mikio HINO, Takehiko OHTA, Kengo SUNADA, and Kunio WATANABE p120-128(1989)"The Numerical Estimation of Floods", Morikita Publication Co., Ltd.